New Astronomy 14 (2009) 341–346

Contents lists available at ScienceDirect

New Astronomy

journal homepage: www.elsevier.com/locate/newast

On some properties of coronal mass ejections in solar cycle 23

Nishant Mittal *, Udit Narain

Astrophysics Research Group, Meerut College, Meerut 250001, India
IUCAA, Post Bag 4, Ganeshkhind, Pune 411007, India

ARTICLE INFO

Article history:
Received 8 July 2008
Received in revised form 19 September 2008
Accepted 15 October 2008
Available online 1 November 2008
Communicated by W. Soon

PACS:
96.60.-j

Keywords:
Sun
Coronal mass ejections
General properties
Solar cycle 23

ABSTRACT

We have investigated some properties such as speed, apparent width, acceleration, latitude, mass and kinetic energy, etc. of all types of coronal mass ejections (CMEs) observed during the period 1996–2007 by SOHO/LASCO covering the solar cycle 23. The results are in satisfactory agreement with previous investigations.

© 2008 Elsevier B.V. All rights reserved.

1. Introduction

The solar cycle and activity phenomena are some of the interesting physical processes that are least understood. Since the discovery of sunspots, their origin and formation with their cycle activity remains a mystery. In a similar way, physics of the recently discovered (compared to dates of sunspots' discovery) solar activity phenomenon, viz; the coronal mass ejections (CMEs) is yet to be understood. Because of CMEs geoeffectiveness and space weather effects that ultimately involve the societal effects on the earth, frequency of their occurrence and other physical parameters such as mass and kinetic energy need to be documented for theoreticians in order to come out with a reasonable CME model.

Coronal mass ejections (see e.g., Cremades and Cyr, 2007; Gopalswamy, 2006; Gopalswamy, 2004; Gopalswamy et al., 2003a,b and references therein) are a topic of extensive study, since they were first detected in the coronagraph images obtained on 1971 December 14, by NASA's OSO-7 space craft (Tousey, 1973). Yashiro et al. (2003) have described properties of Narrow CMEs observed with Large Angle and Spectrometric Coronagraphs (LASCO) on board SOHO (Solar and Heliospheric Observatory). whereas Gopalswamy et al. (2003a) have studied the solar cycle variation of different properties of CMEs such as daily CME rate, average and median speeds and the latitude of solar sources for cycle 23 (1996–2003). Since LASCO/SOHO images the corona continuously since 1996 covering a field of view in the range 1.5–32 R_s, it represents a unique data coverage from solar minimum to maximum and beyond with a single spacecraft (Brueckner et al., 1995).

We have extended the above-mentioned studies for the period 1996–2007. The qualitative results obtained in the present study are expected to be almost the same as those obtained earlier; of course, there might be differences in the numerical estimates.

The data for CMEs have been taken from the catalogue maintained by the Centre for Solar Physics and Space Weather (CSPSW) (http://cdaw.gsfc.nasa.gov/CME_list). The quality index of data taken by us ranges from 1 to 5 scale: poor, fair, typical, good and excellent. Cyr et al. (2000) have suggested that duty cycle correction may not be necessary for the LASCO data.

2. Some properties of CMEs

The *OSO-7* coronagraph detected only 27 CMEs over a period of 19.5 months. The *Skylab* ATM coronagraph recorded 110 CMEs during its 227 days of operation. SOHO/LASCO has detected more than 12900 CMEs over a period of 12-year (January-1996 to December-2007). Table 1 summarizes these observations and updates a previous compilation by Gopalswamy (2004).

* Corresponding author. Address: Astrophysics Research Group, Meerut College, Meerut 250001, India.
E-mail address: nishantphysics@yahoo.com (N. Mittal).

1384-1076/$ - see front matter © 2008 Elsevier B.V. All rights reserved.
doi:10.1016/j.newast.2008.10.004

Table 1
CME properties from various coronagraphs [updated from Gopalswamy (2004)].

Coronagraph	OSO-7	Skylab	Solwind	SMM	LASCO
Epoch	1971	1973–1974	1979–1985	1980, 1984–1989	1996–2007
Field of view (R_s)	2.5–10	1.5–6	03–10	1.6–6	1.2–32
# CME recorded	27	115	1607	1206	12,981
Mean speed (km/s)	–	470	460	350	435
Mean width (deg)	–	42	43	47	41
Mass (10^{15} g)	–	6.2	4.1	3.3	1.2

2.1. Speed of CMEs

Mass motion is the basic characteristic of CMEs which is quantified by their speeds. Coronagraphs obtain images with a preset time cadence. Thus when a CME occurs, the leading edge moves to a greater heliocentric distance. On measuring the heliocentric distance of the leading edge of the CMEs in each LASCO image one obtains CME height as a function of time. It is to be noted that the height–time measurements are made in the sky plane, so all the derived parameters are lower limits to the actual values.

The height–time (h–t) plots fitted to first order polynomials give an average speed within the LASCO field of view; but it may not be suitable for all CMEs. Quadratic fit to the h–t plot gives the constant acceleration which again is an approximation because the acceleration may also change with time (Gopalswamy, 2006). The annual average and median speeds and the average magnitudes of the latitudes of all types of CMEs during the period 1996–2007 are exhibited in Table 2. The overall average and median speeds are 435 km/s and 369 km/s, respectively. The histogram of speeds is in Figs. 1 and 2 exhibits the annual average and median speed distributions. The solar maximum of cycle 23 which falls in the year 2000 coincides with the maximum in speed distribution (cf. Fig. 2). The other maximum in CME mean speed occurs due to the Halloween 2003 CMEs.

Error bars in Fig. 2 show the statistical errors in average and median speeds.

Table 2
Annual average, median speeds and the average magnitude of latitudes of CMEs during 1996–2007 period.

Year	Number of events	Speed (km/s)		Number of events	Average|latitude| (deg)	
		Average	Median		All	$\leqslant\|50°\|$
1996	197	269	237	206	14	13
1997	376	320	272	380	14	12
1998	697	413	361	706	26	20
1999	997	495	436	1002	37	23
2000	1587	501	447	1602	39	25
2001	1483	473	403	1487	35	24
2002	1644	508	450	1659	36	24
2003	1113	544	478	1122	34	24
2004	1084	448	399	1095	28	21
2005	1222	335	361	1238	28	21
2006	1034	321	289	1043	25	20
2007	1441	255	240	1441	25	18

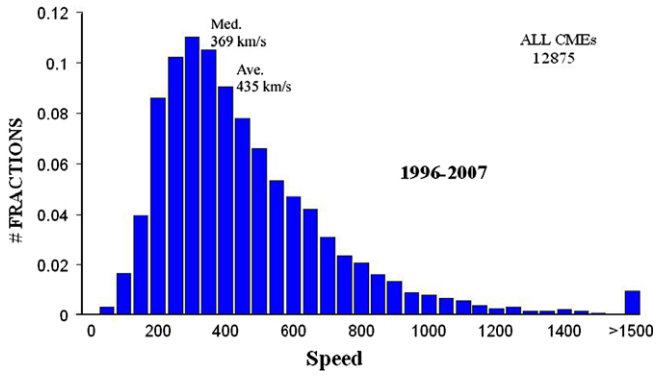

Fig. 1. Histogram shows the speed distribution of all CMEs during 1996–2007. The fractions along y-axis in the figure give the fractional number of events having a given speed.

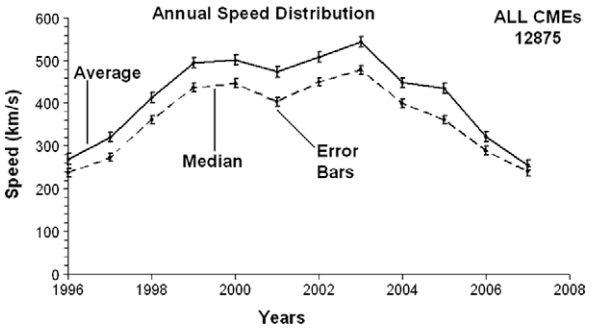

Fig. 2. Annual average and median of CME speeds from 1996 to 2007, showing clear increase towards solar activity maximum.

2.2. CME width

It is measured as the position angle extent in the sky plane. For CMEs away from the limb, the measured width is likely to be an overestimate but it should be true width for CMEs originating from

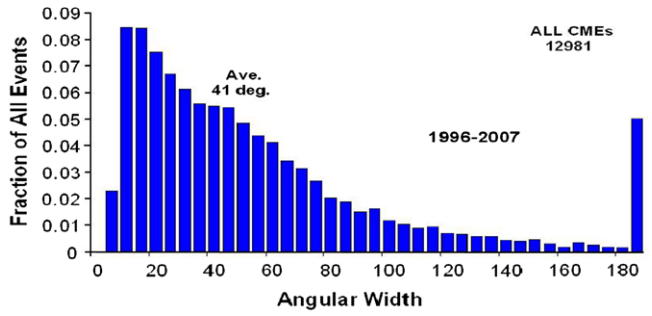

Fig. 3. The width distribution of SOHO/LASCO CMEs from 1996 to 2007. The last bin shows all CMEs with width >180°, which amounts to 5–6% of all CMEs. The fractions in the figure give the fractional number of CMEs having a given angular width.

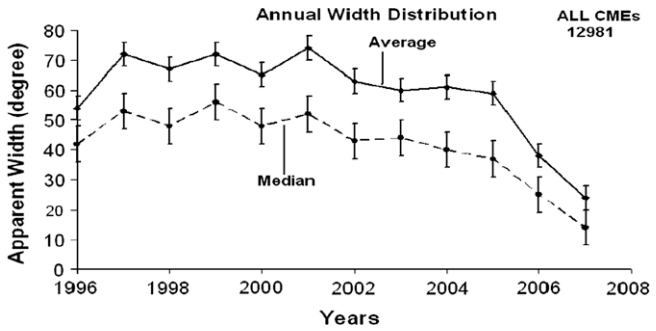

Fig. 4. Annual average and median widths of SOHO/LASCO CMEs from 1996 to 2007 with associated error bars.

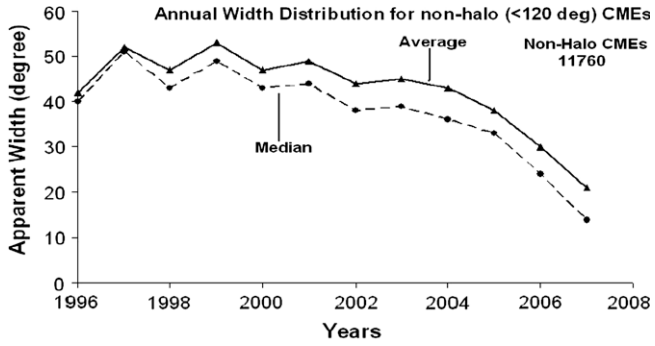

Fig. 5. Annual average and median of non-halo CME widths by SOHO/LASCO from 1996 to 2007.

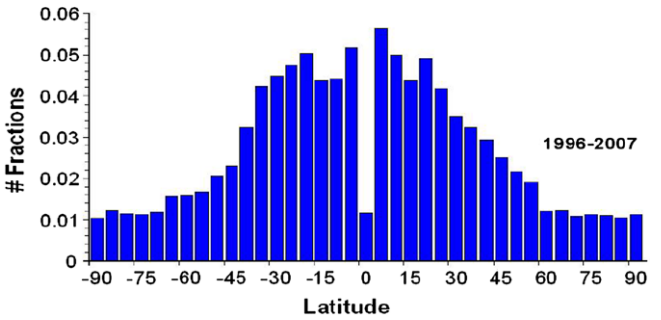

Fig. 6. Histogram shows the latitude distribution of all CMEs from 1996 to 2007. The fractions along *y*-axis in the figure give the fractional number of events having given latitude.

Table 3
Annual median and average CME angular width, along with the associated errors during 1996–2007.

Year	Average	Error of average	Median	Error of median
1996	54	3.8	42	4.8
1997	72	3.7	53	4.6
1998	67	2.8	48	3.5
1999	72	2.1	56	2.6
2000	65	1.8	48	2.3
2001	74	1.9	52	2.4
2002	63	1.7	43	2.1
2003	60	1.9	44	2.4
2004	61	2.1	40	2.6
2005	59	2.2	37	2.8
2006	38	1.5	25	1.9
2007	24	0.8	14	1

close to the limb. Fig. 3 is the histogram of apparent angular width for the period 1996–2007. Fig. 4 exhibits the annual average and median width distribution for the same period. Clearly the width distribution is biased towards lower CME widths. The apparent angular width of CMEs ranges from a few degrees to more than 120° (cf. Fig. 3).

The average width from the 12-year data for non-halo CMEs (11,760) is 41° and the median width is 36°. Halo-CMEs are those CMEs with width >120°, but they are excluded because it is difficult to measure the actual width of such halo-CMEs due to projection effect. The average width for all CMEs is smallest during solar minimum (1996 and 2007). The trend of variation is quite similar (cf. Figs. 4 and 5). The peak in width occurs around the year 1999 and declines slowly to minimum similar to Yashiro et al. (2004)).

The statistical errors in annual width distribution are exhibited in Fig. 4. For completeness their numerical values are exhibited in Table 3.

2.3. Latitudes

The latitude distribution of the central position angles of CMEs tends to cluster about the equator at minimum but broadens to cover all latitude near solar maximum. The latitude distribution of CMEs depends on the distribution of closed field regions on the solar surface (Hundhausen, 1993). The CME latitude is obtained from the central position angle of the CME under the assumption that CME propagates radially away from the solar source region (Hundhausen, 1993; Gopalswamy et al., 2003b). This assumption may not be valid during solar minimum periods when the CME path may be controlled by the global dipolar field of the Sun.

During the rising phase of cycle 23 (1997–1998), the CME latitudes were generally close to the equator and subsequently spread to all latitudes. During the maximum phase there are many polar CMEs and the number of such CMEs was larger in the southern hemisphere and occurred over a longer time period than in northern hemisphere.

Fig. 6 shows distribution of apparent latitude for the 12-year (1996–2007) period involving 12981 CMEs. Table 2 exhibits annual averages of latitudes of all CMEs and those having latitudes $\leqslant|50°|$.

It is clear from Fig. 6 that a very few CMEs are ejected from close to the equator. The distribution is almost symmetrical about the equator. During 1996–2007 period the number of CMEs having latitudes in between ±5° and ±35° is much larger than those beyond ±35°.

2.4. CME acceleration

All CMEs have positive acceleration in the beginning as they lift off from rest. In this situation the propelling force, exceeds gravity force and other restraining forces. As soon as a CME lifts off, it is subject to an additional retarding force (the drag), F_d, which is given by (Cargill et al., 1996; Gopalswamy, 2004)

$$F_d = C_d A\rho - V_{\mathrm{CME}} - V_{\mathrm{SW}} - (V_{\mathrm{CME}} - V_{\mathrm{SW}}),$$

where C_d is the drag coefficient, A is the surface area of the CME, ρ is the plasma density, V_{CME} is the CME speed and V_{SW} is the solar wind speed. Close to the Sun, the solar wind speed is negligible.

Fig. 7 is the histogram of CME acceleration for the period 1996–2007, i.e. of cycle 23. It is clear from this figure that a majority (66%) of CMEs are decelerated, about 9% of them move with little acceleration and the remaining 25% have positive acceleration. Thus CMEs have clear bias towards negative acceleration (deceleration). In all there are 7995 CMEs whose acceleration could be determined.

The *h*–*t* plots fall into three types: accelerating, constant speed and decelerating, indicating different degrees of propelling and retarding forces acting on CMEs (Gopalswamy et al., 2001). The accelerating profile indicates that the propelling force is still active

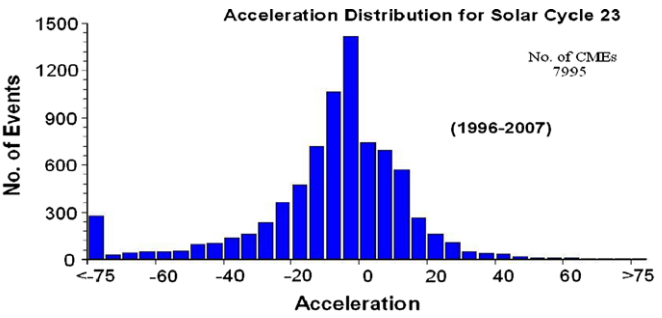

Fig. 7. Histogram of acceleration of CMEs, showing clear bias towards deceleration.

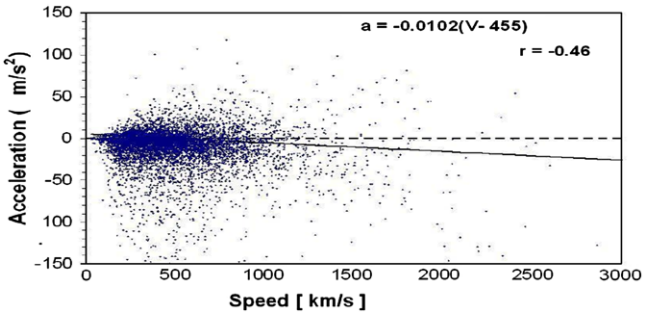

Fig. 8. Acceleration as a function of speed of all CMEs from 1996 to 2007. The acceleration has a large scatter, but there is a clear trend that the fast CMEs decelerate, while slow CMEs accelerate. "*r*" is the correlation coefficient of the distribution.

in pushing the CME outward. Fig. 8 shows a scatter plot between the measured acceleration, a (in m/s^2) and speed, V (in km/s) of all the CMEs for which the acceleration estimate was possible. Despite the large scatter, the acceleration has a reasonable correlation with speed, $a = -0.0102\ (V - 455)$, which shows that slow CMEs ($V < 455$ km/s) accelerate, CMEs of intermediate speed ($V \sim 455$ km/s) have no appreciable acceleration and fast CMEs (>455 km/s) decelerate. Close to the Sun "a" is determined by the propelling force, gravity and coronal drag. If $a = 0$, then $V = 455$ km/s.

2.5. Mass and energy

The width is a good indicator of the mass content of CMEs. The mass in a CME is estimated by determining the CME volume and the number of electrons in the CME under the assumption that the CME is fully ionized hydrogen plasma with 10% Helium.

The current LASCO database of CMEs contains more than 12,000 events. CME observations are available over a significant part of solar cycle; thereby allowing us to obtain a very reliable estimate of their mass and energy profiles.

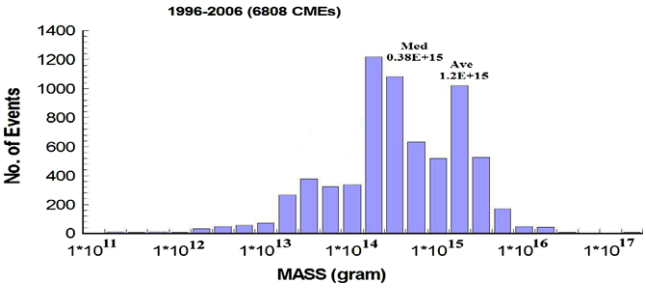

Fig. 9. CME mass of SOHO CMEs for the period 1996–2006.

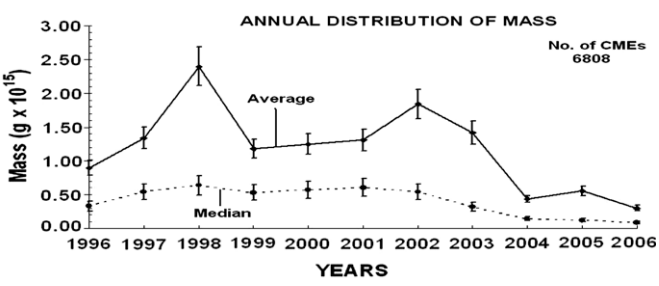

Fig. 10. Annual average and median of CME mass (g) by SOHO/LASCO from 1996 to 2006, with statistical error bars.

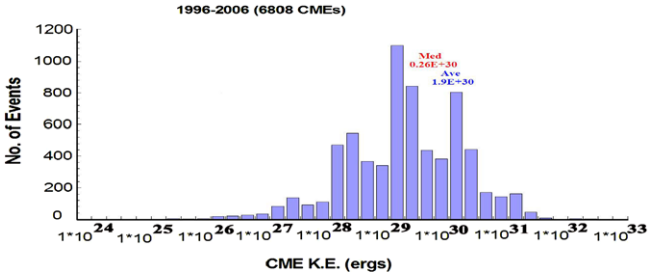

Fig. 11. CME kinetic energy of SOHO CMEs for the period 1996–2006.

Fig. 9 is an 11-year (solar cycle 23) histogram involving CME mass and corresponding number. The annual average and median mass and kinetic energy are exhibited in Figs. 10 and 12. The average mass of all types of CMEs (total number 6808) is found to be about 1.2×10^{15} g. The total mass ejected in CMEs range from a few times 10^{11} g to more than 10^{17} g. The LASCO/SOHO averages are approximately lower by a factor of two than those of Solwind and SMM averages confirming the results in Cremades and Cyr, 2007.

Fig. 11 is the histogram of kinetic energy of all types of (6808) CMEs observed during solar cycle 23. The kinetic energy obtained from the measured speed and mass ranges from $\sim 10^{27}$ erg to 10^{32} erg with an average value of 1.9×10^{30} erg. Some very fast and wide CMEs have kinetic energies exceeding 10^{33} erg and they generally originate from large active regions and are accompanied by powerful flares (Gopalswamy et al., 2005). There are lots of uncertainty in estimating mass and energy of CMEs. Hence the vertical error bars are over plotted in Figs. 10 and 12.

2.6. Occurrence rate

A CME rate of 0.5 CME/day was derived from the OSO-7 coronagraph data (Tousey et al., 1974). Skylab data indicated an average rate of ~1/day with good correlation between sunspot number (SSN) and CME rate (Hildner et al., 1976). Combining Skylab, SMM, Helios (Photometer) and Solwind observations Webb and Howard (1994) found a rate of 0.31 to 0.77 CME/day for the solar minimum years and 1.75 to 3.11 CMEs/day for the solar maximum years. The correlation between CME rate and SSN was also found to hold when the data were averaged over Carrington Rotation (CR) periods (Cliver et al., 1994). Based on the first two years of operation of SOHO Cyr et al. (2000) studied the CME rate and found them to increase steadily during the rise phase of the solar cycle. They concluded that the rate corresponding to the rise phase of cycle 23 was not significantly different from pre-SOHO observations.

During solar minimum, one CME occurs every other day. The rate goes up to several per day during solar maximum. On one day during solar maximum, 13 CMEs were recorded by SOHO;

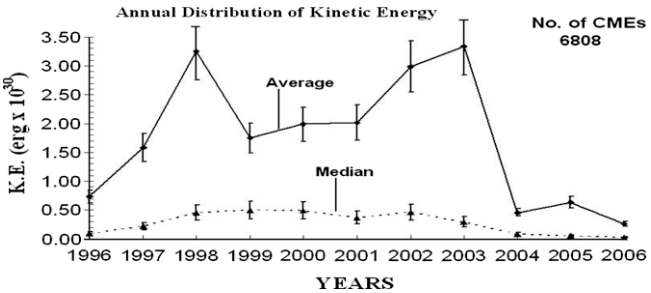

Fig. 12. Annual average and median of CME K.E. (erg) by SOHO/LASCO from 1996 to 2006, with statistical error bars.

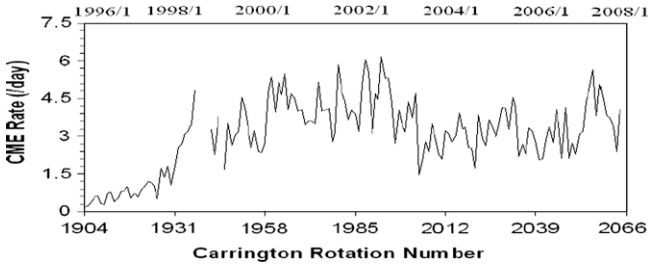

Fig. 13. CME rate averaged over Carrington Rotation (CR) periods. The gap in the CME rate is due to SOHO mission interruption during June–October 1998 and a smaller gap during January–February, 1999.

there were several days with more than 10 CMEs (Gopalswamy et al., 2003a). The daily CME rate averaged over Carrington Rotation (27.3 days), increases from less than 1 during solar minimum in 1996 to slightly more than 6 during maximum (2000) (Fig. 13). The large spikes are due to active regions that are very active producers of CMEs.

However the SOHO years reveal a much sharper increase of activity in year 1998. It must be taken into account that the values for this year are the most uncertain ones, due to two large data gaps that account for almost 6-month. The years 2004–2007 do not show appreciable decline in the CME production, despite the quick decrease in the solar activity and represents a new result. Only future data may confirm this trend.

The solar maximum rate of SOHO CMEs was nearly twice the highest corrected rate (3.11/day) reported for previous cycles (Webb and Howard, 1994). We attribute this primarily to the better sensitivity and the enormous dynamic range (16000:1) of the LASCO coronagraph. Additional factors include large field of view and more uniform coverage over long periods of time (Howard et al., 1997). Note that the LASCO CME rate is not corrected for duty-cycle, but an analysis by Cyr et al. (2000) suggested that such a correction may not be necessary for the LASCO data. During the maximum of solar cycle 23, the CME rate exhibits two peaks one in 2000 and second in 2002. This was also discussed by Gopalswamy (2004); who in addition compares the location of the two peaks in both CME rate and SSN averaged over Carrington Rotation periods.

2.7. Halo CMEs

Halo CMEs are so named because they appear to surround the occulting disk of the coronagraph (Howard et al., 1982). CMEs heading toward and away from the observer can appear as halos. Only those halo CMEs, which are directed towards the Earth, are geoeffective and can produce geomagnetic storm, etc. at Earth. The CMEs having angular width >180° are considered as halo-CMEs.

Fig. 14 exhibits sunspot number, number of halo and fast and wide CMEs. It is clear from the figure that the solar maximum peak and halo CME peak occurs at the year 2000. The peak in number of fast and wide CMEs occurs at years 2002 and 2005. There are two peaks in the number of halo CMEs also. Thus the occurrence of halo or fast and wide CMEs is not well correlated with solar cycle variation.

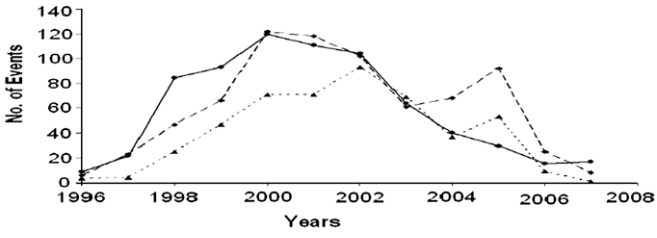

Fig. 14. Figure shows comparison between sunspot numbers, halo CMEs and fast and wide CMEs. Solid line represents sunspot number, dashed line represents halo CMEs and dotted line (with triangles) shows fast and wide CMEs.

The number of halo CMEs is minimum (06) at the solar minimum (1996) and maximum (122) at solar maximum (year 2000). The situation is somewhat similar at the other solar minimum year (2007).

3. Discussion and conclusions

The histogram of CME speed (Fig. 1) and annual (average and median) speed distributions show that there is bias towards low speed CMEs. There is one peak near solar maximum (year 2000) and another peak around the year 2003 (cf. Fig. 2). The second peak is due to super-active regions which are prolific producers of (Halloween 2003) CMEs.

The histogram of apparent width (Fig. 3) for non-halo CMEs and the annual average and median apparent width distribution (Fig. 4) for all types of CMEs show bias towards lower apparent widths (25°–55°). The variation of apparent width with solar activity (sunspot number) is not quite clear but the apparent width does decline at solar minimum (years 1996 and 2007).

Around solar minimum the CMEs tend to occur at lower latitudes, and as the rise to maximum occurs, the apparent latitude increases. The CME apparent latitudes are well-correlated with the latitude distribution of the helmet streamers (Hundhausen, 1993), rather than with the "butterfly diagram" latitudes of active regions (Hudson et al., 2006). The histogram of latitude (Fig. 6) shows a two-lobe distribution with distinct peaks at mid-latitudes (about 35°) in both the northern and southern hemispheres and relatively few events near the equator. This is very different to the latitude distribution of white-light CMEs, which is sharply peaked at low latitudes.

The histogram of CME acceleration (Fig. 7) shows bias towards negative acceleration. About 66% have negative acceleration, 25% have positive acceleration and the remaining 9% have very little acceleration.

The mass is estimated as the excess mass in the coronagraphic field of view assuming that the entire mass is located in the sky plane (Vourlidas et al., 2002). Mass estimates have also been made using radio (Gopalswamy and Kundu, 1993; Ramesh et al., 2003) and X-ray observations (Rust and Hildner, 1976; Hudson et al., 1996; Sterling and Hudson, 1997; Gopalswamy and Hanaoka, 1998). The radio and X-ray estimates (10^{14}–10^{15} g) are generally lower than the white-light mass values. This is due to the fact that the X-ray and radio mass estimates correspond to the regions close to the Sun (and involve thermal emission properties of CME plasma) whereas the white light estimates correspond to larger heights (and involve Thomson scattering).

The histogram of CME mass (Fig. 9) and the annual average and median distribution of mass (Fig. 10) show that it has no clear relation with solar cycle variation except for the fact that the annual average or median mass is lowest at solar minimum (year 2006). There are three peaks in annual mass distribution (cf. Fig. 10) at the years 1998, 2002, and 2005 in descending order of magnitude.

The histogram of CME kinetic energy (Fig. 11) and the annual average and median kinetic energy distribution (Fig. 12) is similar to those of mass.

The matter presented above leads us to conclude the following:

1. LASCO/SOHO observed 12981 CMEs of all types during the period 1996–2007 forming solar cycle 23. Out of these 737 (5.7%) are halo CMEs. The number of fast and wide CMEs is 484 (3.7%).

2. The average and median CME speeds of all types are 435 km/s and 369 km/s, respectively. The average CME speed of all types of CMEs obtained by Gopalswamy (2006) for the data from 1996 to June 2005 is 483 km/s which differs from the present value by about 10%.
3. The annual average CME speed variation is consistent with solar cycle 23 variations except for the second peak which occurs because of Halloween 2003 CMEs, as expected.
4. The apparent CME width distribution is biased towards lower widths. The average apparent width for non-halo (width $\leqslant 120^\circ$) 11,760 CMEs obtained by us is 41°. The corresponding width for 8690 CMEs obtained by Gopalswamy (2006) is 46°.
5. Out of 7995 CMEs, whose acceleration was available, about 66% have negative acceleration, 25% have positive acceleration and the remaining 9% have very little acceleration. The distribution was biased towards CMEs which decelerated. The correlation coefficient for acceleration vs. speed is found to be satisfactory.
6. The mass and kinetic energy of only 6808 CMEs could be determined. The average values of mass and kinetic energy are 1.2×10^{15} g and 1.91×10^{30} ergs, respectively. The corresponding values obtained by Gopalswamy (2006) are 6.7×10^{14} g (with 4124 CMEs) and 5.4×10^{29} ergs (with 4133 CMEs).
7. About 48% of all CMEs come from northern hemisphere and about 51% come from southern hemisphere. Only 1% of CMEs come from equatorial region.
8. CME rate per day (averaged over Carrington Rotation) increases from about 0.5 in 1996 to more than 3 in 1999. It is about 5 in 2000, is more than 6 in 2002, remains more than 3 from 2003 onwards and is about 6 in 2007. It does not decline near next solar minimum (2006–2007). It represents a new result and can be confirmed by the data available in future during cycle 24.
9. The variation in the number of halo or fast and wide CMEs is not well-correlated with the solar cycle variation.

Acknowledgements

We are thankful to Meerut College authorities for their help and encouragement. We are also thankful to HRI, Allahabad library for some relevant literature. We are also thankful to HRI, Allahabad for providing some financial assistance to one of the author. We are highly grateful to N. Gopalswamy and P.K. Manoharan for many helpful correspondences. SOHO/LASCO CME catalog is generated and maintained at the CDAW Data Center by NASA and The Catholic University of America in cooperation with the Naval Research Laboratory. SOHO is a project of international cooperation between ESA and NASA. The authors would like to thank for the excellent LASCO-CME catalogue, from which the data have been taken. The authors are very much grateful to the learned referees for improving the manuscript through their enlightening comments.

References

Brueckner, G.E. et al., 1995. Sol. Phys. 162, 357.
Cargill, P.J., Chen, J., Spicer, D.S., Zelesak, S.T., 1996. J. Geophys. Res. 101 (A3), 4855.
Cliver, E.W., Cyr St., O.C., Howard, R.A., McIntosh, P.S., 1994. In: Rusin, V., Heinzel, P. (Eds.), Vial, Solar Coronal Structures. VEDA Publishing House of the Slovak Academy of Sciences (p. 83).
Cremades, H., Cyr St., O.C., 2007. Space Res. 40, 1042.
Cyr St., O.C. et al., 2000. J. Geophys. Res. 105 (A8), 18169.
Gopalswamy, N., 2004. In: Poletto, G., Suess, K.T. (Eds.), In the Sun and the Heliosphere as an Integrated System. Kluwer. p. 201.
Gopalswamy, N., 2006. Astrophys. Astron. 27, 243.
Gopalswamy, N., Hanaoka, Y., 1998. ApJ 498, L179.
Gopalswamy, N., Kundu, M.R., 1993. Sol. Phys. 143, 327.
Gopalswamy, N., Yashiro, S., Kaiser, M.L., Howard, R.A., Bougeret, J.-L., 2001. J. Geophys. Res. 106 (A12), 29219.
Gopalswamy, N., Lara, A., Yashiro, S., Nunes, S., Howard, R.A., 2003a. In: Wilson, A. (Ed.), In Solar Variability as an Input to the Earth's Environment ESA SP-535. ESA, Publication division, Nooedwijk, pp. 403–414.
Gopalswamy, N., Shimojo, M., Lu, W., Yashiro, S., Shibasaki, K., Howard, R.A., 2003b. ApJ 586, 562–578.
Gopalswamy, N., Yashiro, S., Liu, Y., Michalek, G., Vourlidas, A., Kaiser, M.L., Howard, R.A., 2005. J. Geophys. Res. 110, A09S15.
Hildner, E., Gosling, J.T., MacQueen, R.M., Munro, R.H., Poland, A.I., Ross, C.L., 1976. Sol. Phys. 48, 127.
Howard, R.A. et al., 1997. In: Crooker, N., Joselyn, J., Feynman, J. (Eds.), Coronal Mass Ejections, AGU Monography. American Geophysics Union, Washington DC, p. 17.
Howard, R.A., Michels, D.J., Sheeley Jr., N.R., Koomen, M.J., 1982. ApJ 263, L101.
Hudson, H., Acton, L.W., Freeland, S.L., 1996. ApJ 470, 629.
Hudson, H.S., Bougeret, J.-L., Burkepile, J., 2006. Space Sci. Rev. 123, 13–30.
Hundhausen, A.J., 1993. J. Geophys. Res. 98, 13177.
Ramesh, R., Kathiravan, C., Sastry, C.V., 2003. Metric radio observations of the evolution of a "Halo" coronal mass ejection close to the sun. ApJ 591, L163.
Rust, D.M., Hildner, E., 1976. Sol. Phys. 48, 381.
Sterling, A., Hudson, H., 1997. YOHKOH SXT observations of X-ray "Dimming" associated with a halo coronal mass ejection. ApJ 491, L55.
Tousey, R., 1973. The solar corona. Space Res. 13 (2), 713–730.
Tousey, R., Howard, R.A., Koomen, M.J., 1974. Bull. Am. Astron. Soc. 6, 295.
Vourlidas, A., Buzasi, D., Howard, R.A., Esfandiari, E., 2002. In: Wilson, A. (Ed.), Solar variability: from core to outer frontiers, vol. 1. ESA Publications Division, ESA SP-506, Noordwijk, p. 91.
Webb, D.F., Howard, R.A., 1994. J. Geophys. Res. 99 (A3), 4201.
Yashiro, S., Gopalswamy, N., Michalek, G., Howard, R.A., 2003. Adv. Space Res. 32, 2631.
Yashiro, S., Gopalswamy, N., Michalek, G., Cyr St., O.C., Plunkett, S.P., Rich, N.B., Howard, R.A., 2004. J. Geophys. Res. 109, A07105.